Abdominal Radiology

Published online: 25 November 2017

Abdom Radiol (2018) 43:1101–1119
https://doi.org/10.1007/s00261-017-1385-z

The bottom line: MRI and CT findings of unusual rectal and perirectal pathology

Stephanie Font, Candice Bolan, Melanie Caserta

Division of Diagnostic Radiology, Mayo Clinic, 4500 San Pablo Road South, Jacksonville, FL 32224, USA

Abstract

Although common nonspecific symptoms (i.e., rectal bleeding, pelvic pressure, and change in bowel habits) are associated with rectal cancer, occasionally these are related to a different underlying disease. Over the past few years, considerable progress has been made in imaging of the rectum. Specifically, new magnetic resonance techniques and capabilities provide impressive high-resolution assessment of the rectal wall and enable evaluation and characterization of the perirectal tissues. This paper reviews imaging findings of uncommon causes of rectal and perirectal pathology that may be clinically confounded with rectal cancer. Radiologists need to be aware of uncommon pathologies in this region in order to facilitate optimal management decisions.

Key words: MR—Perirectal mass—Presacral mass—Rectal mass

The rectal and perirectal space is clinically important and relevant to multiple disciplines. Magnetic resonance imaging (MRI) is the preferred modality for assessing rectal and perirectal masses due to high soft tissue contrast and the ability to demonstrate the layers of the rectal wall. The anatomy in this region is complex, and it is important to understand the relationship with adjacent organs. In females, the vagina and cervix are located anterior to the rectum, while in males, the prostate and seminal vesicles lie anteriorly. Much of the rectum is extraperitoneal, although the upper third is covered anteriorly and laterally by the peritoneal reflection [1]. The presacral space, sacrum, and coccyx form the posterior boundary (Fig. 1). These adjacent organs serve as potential sources of unusual rectal and perirectal pathology.

Although rectal adenocarcinoma account for the vast majority (98%) of rectal cancers [2], a wide variety of rectal and perirectal conditions can mimic primary rectal cancer. Over the past few years, significant progress has been made in imaging of the rectum and regional structures. Specifically, new MRI techniques provide impressive high-resolution assessment of the rectal wall and enable evaluation and characterization of the perirectal tissues. The multiplanar capability of MR also helps in lesion localization and characterization.

In this pictorial essay, imaging findings of uncommon causes of rectal and perirectal pathology that may be clinically confounded with rectal cancer are reviewed. The entities discussed can be broadly classified by location: rectal wall, perirectal/presacral space, and sacrum (Table 1).

Rectal wall

There are many types of benign and malignant lesions that can involve the rectal wall and simulate rectal adenocarcinoma as listed in Table 1.

Rectal gastrointestinal stromal tumor

Gastrointestinal stromal tumor (GIST) is the most common mesenchymal neoplasm of the gastrointestinal tract [3, 4]. The most common location for GIST is the stomach (70%) followed by the small bowel (20%–25%). The rectum is the third most commonly involved part of the gastrointestinal tract (5%–7%) [5, 6]. GISTs are thought to derive from a precursor of the interstitial cells of Cajal, normally present in the myenteric plexus, and are clearly distinct from other mesenchymal tumors, such as leiomyomas or leiomyosarcomas [7]. Most can be distinguished histologically by the expression of membrane receptor c-kit. Some authors support stratifying GIST into very low-, low-, intermediate-, and high-risk categories rather than benign or malignant [8, 9]. Most affected individuals are over 50 years of age at time of presentation.

CME activity This article has been selected as the CME activity for the current month. Please visit https://ce.mayo.edu/node/56624 and follow the instructions to complete this CME activity.

Correspondence to: Candice Bolan; *email:* Bolan.Candice@mayo.edu

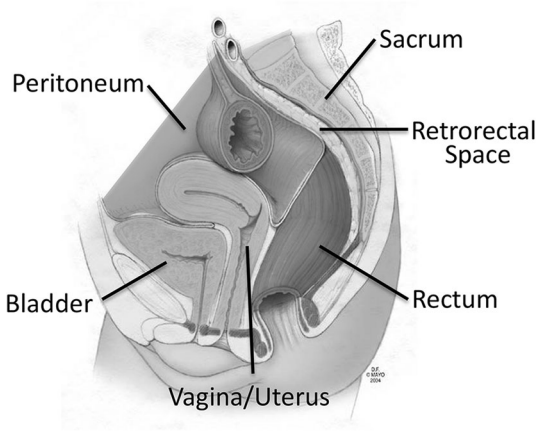

Fig. 1. Illustration outlines the different potential sources and locations of unusual rectal and perirectal pathology. Used with permission of Mayo Foundation for Medical Education and Research, all rights reserved.

There is no consensus in the literature regarding gender predilection. Although clinical presentation depends on size and site of tumor, abdominal pain or distention is the most common presentation followed by bleeding or unexplained anemia [10].

Radiologic features also vary depending on tumor size. Most GISTs demonstrate exophytic growth, as they arise from the muscularis propria [9]. They tend to be large, hypervascular, enhancing masses and are often heterogeneous because of necrosis, hemorrhage, and/or cystic degeneration. When located in the rectal region, GIST may present as a focal circumscribed mass with rectal wall expansion (Fig. 2). Other submucosal mesenchymal tumors such as schwannoma and leiomyoma can be difficult to distinguish from GIST on the basis of imaging alone.

MRI can better demonstrate the heterogeneous nature given superior soft tissue contrast resolution in comparison to CT (Fig. 3). Rectal GISTs typically

Table 1. Unusual rectal and perirectal pathology by location

Rectal wall	Perirectal/presacral space	Sacrum
Mesenchymal mass	Developmental cysts	Teratoma
Gastrointestinal stromal tumor	Retrorectal cystic hamartoma/tailgut cyst	Chordoma
Leiomyoma	Rectal duplication cyst	Schwannoma
Lipoma	Epidermoid cyst	Neurofibroma
Hemangioma	Dermoid cyst	Anterior meningocele
Schwannoma	Neurenteric cyst	Sarcoma (ewing, osteosarcoma, chondrosarcoma)
Myofibroblastic sarcoma	Neurogenic mass	Benign osseous lesions (giant cell tumor, osteoma, bone cyst)
Neuroendocrine tumor	Extramedullary hematopoiesis	
Lymphoma	Mesenchymal mass	
Metastasis	Gynecologic pathology	
Melanoma	Endometriosis	
Colitis cystica profunda	Ovarian	
	Peritoneal pathology	
	Multicystic benign mesothelioma	
	Metastasis	

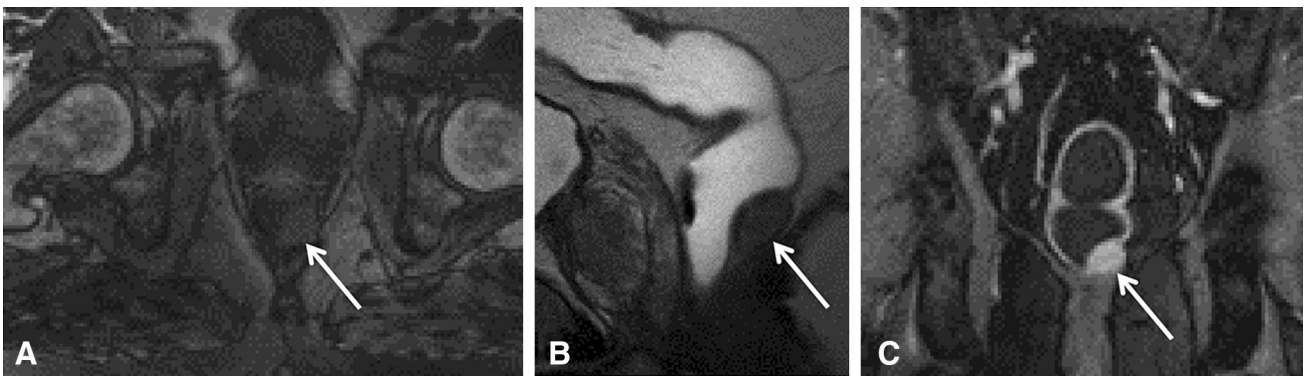

Fig. 2. Surgically proven distal rectal GIST. **A** Axial T1-weighted image shows a well circumscribed intermediate T1 signal intensity rectal wall mass (arrow). **B** Sagittal T2-weighted with rectal gel in place illustrates the exophytic nature of the mass (arrow). Interestingly the T2 signal is intermediate to low intensity which is atypical for GIST. Leiomyoma is also in the differential diagnosis. **C** Fat-saturated T1-weighted post-contrast coronal image shows avid enhancement (arrow).

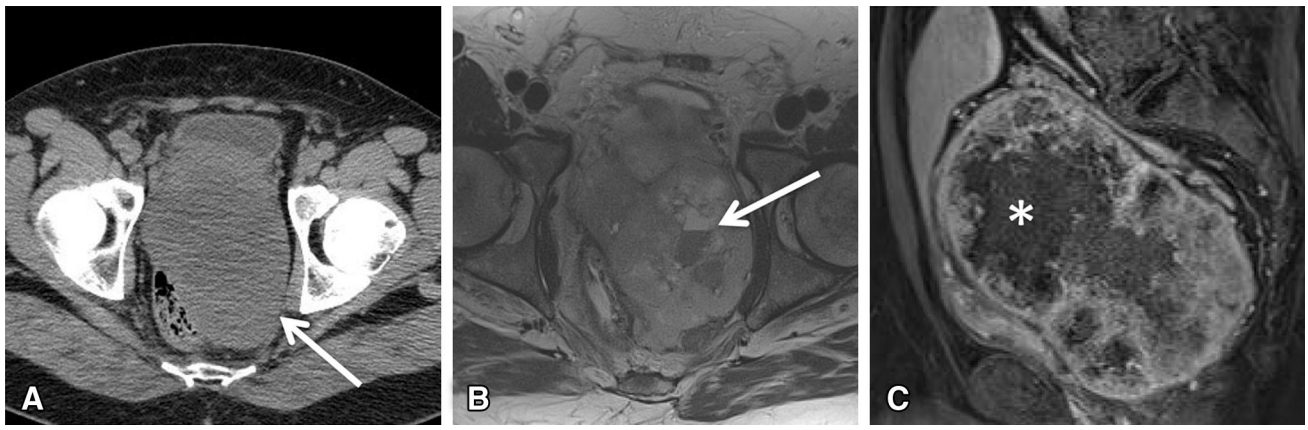

Fig. 3. Surgically proven rectal GIST. **A** Axial unenhanced CT shows a large circumscribed soft tissue mass (arrow) in the left rectal wall. **B** Axial T2-weighted image shows the complexity of the lesion with variable signal intensity. Note the fluid level with low signal intensity layering hemorrhage (arrow). **C** Sagittal post-contrast fat-saturated T1-weighted MR image shows heterogeneous enhancement of the mass with central necrosis (asterisk).

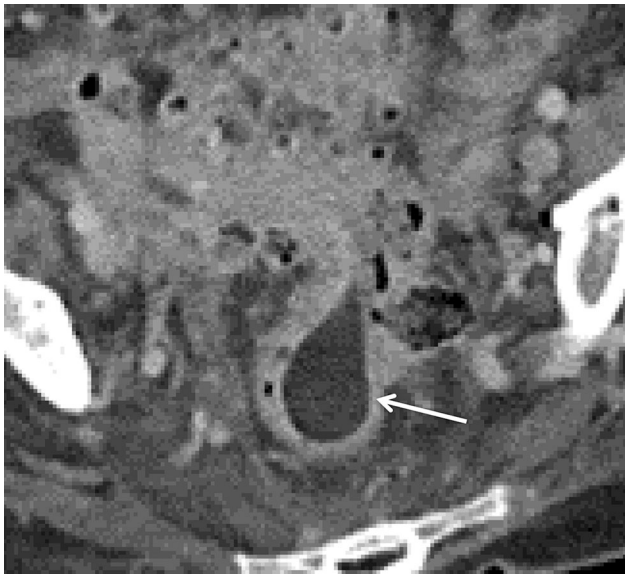

Fig. 4. Rectal Lipoma. CT easily demonstrates the fatty nature of this smooth walled submucosal lipoma (arrow).

demonstrate uniform intermediate signal intensity on T1-weighted images, are variably hyperintense on T2-weighted images, and show marked heterogeneous contrast enhancement [6, 11]. Calcifications may be seen in the setting of prior bleeding episodes or due to tumor necrosis with cystic degeneration. Some features that may differentiate rectal GISTs from other rectal diseases include prominent extraluminal location, no surrounding lymphadenopathy, and lack of bowel lumen constriction despite large size of the lesion [12].

The most common sites for metastases are the liver and peritoneal cavity [5]. Unlike gastrointestinal adenocarcinomas, GISTs metastasizing to lymph nodes is extremely rare [7]. Treatment options include surgical excision and c-kit inhibitor therapy.

Lipoma

Lipoma is the most frequently encountered submucosal tumor in the colon, but it is the second most common benign tumor in the rectum after leiomyoma. Lipomas originate in the wall superficial to the muscularis propria. These are usually broad based with smooth margins, but can occasionally become pedunculated [6]. Both CT and MRI readily demonstrate the fat content of the mass (Fig. 4). On MRI, the mass is isointense to subcutaneous fat on all sequences and will demonstrate low signal intensity on fat suppressed images.

Hemangioma

Large intestine cavernous hemangiomas are rare, but most often involve the rectosigmoid region. Rectal bleeding is the most common clinical presentation. Rectal hemangioma may be a solitary isolated finding or may be associated with Klippel–Trenaunay–Weber syndrome [13]. The presence of phleboliths is a key imaging feature. Calcification of phleboliths is readily apparent on CT imaging. Phleboliths appear as low signal intensity foci on both T1- and T2-weighted images [11].

Klippel–Trenaunay–Weber syndrome can be diagnosed when at least two of the following features are

demonstrated: capillary malformations (usually port-wine stains), soft tissue or bone hypertrophy, and varicose veins or venous malformations [14]. Involvement of the gastrointestinal tract is uncommon, occurring in only 20% of patients [15]. Bleeding is the most common reported symptom in Klippel–Trenaunay–Weber syndrome with gastrointestinal involvement [16, 17]. The distal colon and rectum are the most frequently involved sites [16, 17].

In a reported case by Cha et al. [15], CT showed marked mural thickening of the sigmoid colon and rectum, with varices and associated phleboliths. MRI helps delineate the extent of extremity, intra-abdominal, and pelvic involvement. Varicose vessels can be seen as serpentine flow voids on T2-weighted images, with associated enhancement on post-contrast imaging (Fig. 5).

Rectal carcinoid

Gastrointestinal carcinoids are currently referred to as gastroenteropancreatic neuroendocrine tumors. The small bowel is the most common location for gastrointestinal carcinoid. The rectum is the second most common site followed by the appendix. Carcinoid of the rectum and appendix are often discovered incidentally and are typically small lesions with a low risk for

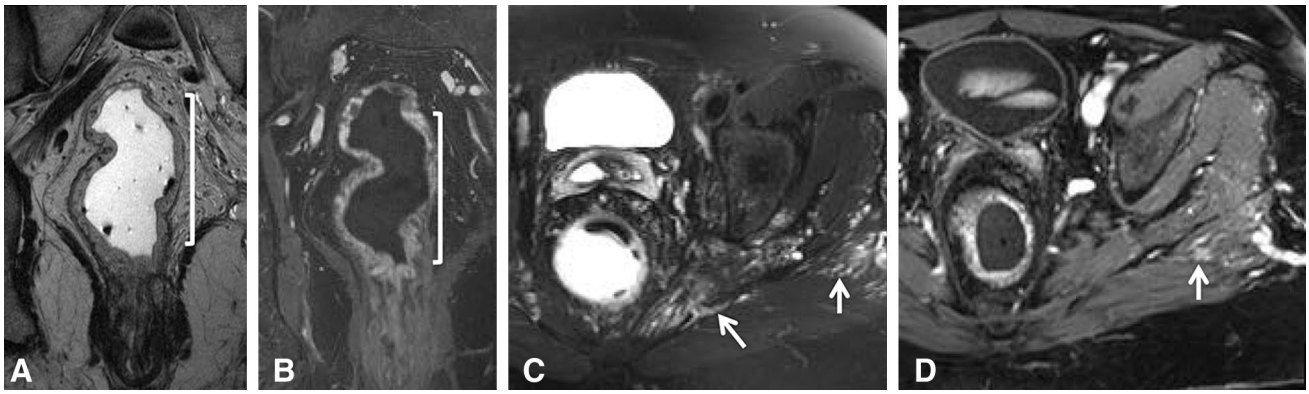

Fig. 5. Rectal wall hemangioma in a patient with Klippel–Trenaunay–Weber syndrome. Rectal gel is present on all images. **A** Coronal T2-weighted image shows multiple flow voids (bracketed) within the rectal wall that also enhance, as seen on **B** coronal T1-weighted post-contrast image. These are compatible with ectatic veins. **C** Axial T2-weighted fat-saturated image shows additional T2 hyperintense serpentine structures extending to the left gluteal soft tissues (arrows). Enhancement of the dilated rectal and left gluteal vessels is appreciated on **D** axial post-contrast image.

Fig. 6. Surgically proven rectal carcinoid. **A** Axial T2-weighted fat-saturated image shows a discrete submucosal lesion (arrow) with intermediate T2 signal. **B** Post-contrast and **C** subtraction images shows evidence of enhancement.

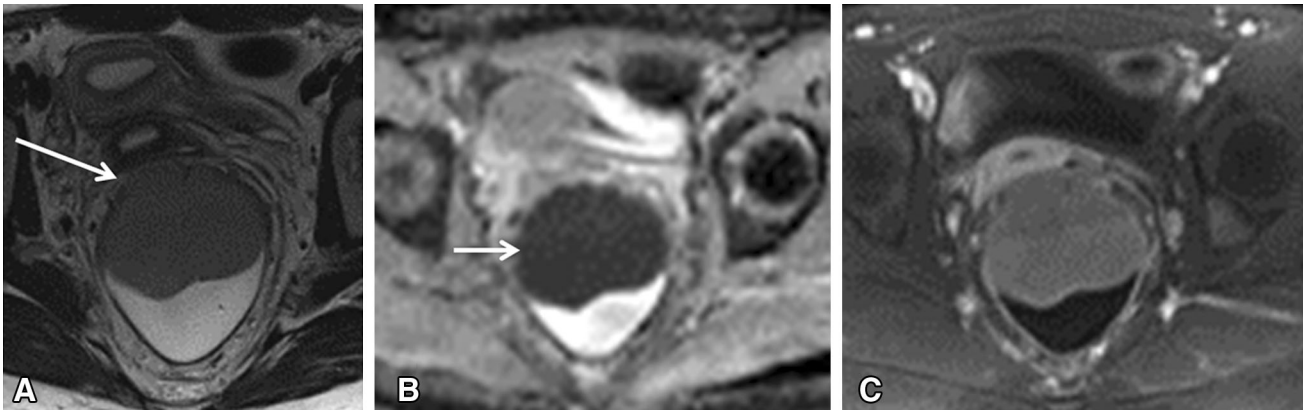

Fig. 7. Biopsy proven rectal lymphoma. **A** Axial T2-weighted image with rectal gel demonstrates a homogeneous intermediate to mildly hyperintense intraluminal rectal mass with loss of the low T2 signal muscularis propria (arrow). **B** Apparent diffusion coefficient map demonstrates markedly low signal (arrow), a feature of lymphoma. **C** Post-contrast axial T1-weighted image with fat suppression illustrates homogeneous low level enhancement.

metastasis [18]. They are epithelial tumors that develop in the deep portions of glands, typically invading through the muscularis mucosa into the submucosa, and resembling submucosal tumors [19].

In general, the mean age of patients at diagnosis is 56.2 years [18], and there appears to be no gender predilection. Most patients are asymptomatic at the time of presentation. Although carcinoid syndrome is frequently related to carcinoid tumors, the classic symptoms of flushing, diarrhea, abdominal pain, and occasional asthma or right-sided cardiac valvular problems are actually uncommon. Midgut primary tumors appear to be more hormonally active than distal rectal carcinoids [20].

Small carcinoids may be difficult to delineate on CT; however, on MRI they appear as a discrete mass or asymmetrical rectal wall thickening. They are isointense to muscle on T1-weighted images, iso- to hyperintense on T2-weighted images (Fig. 6), and show homogeneous contrast enhancement [5].

Minimally invasive surgery is an option for localized small tumors (< 1 cm). Different treatment strategies are considered when there is evidence of regional invasion or metastatic disease.

Lymphoma

Primary rectal lymphoma is rare (0.05% of all primary rectal malignancies) and the clinical presentation is often indistinguishable from rectal carcinoma. Risk factors include human immunodeficiency virus (HIV) infection, immunosuppression after solid organ transplantation, and inflammatory bowel disease [21, 22]. Findings of rectal lymphoma are similar to lymphoma elsewhere in the gastrointestinal tract, often presenting with a bulky mass. One distinguishing feature of lymphoma is the lack of obstruction in the presence of a large mass. Preservation of the mesorectal fat plane is also more likely with lymphoma compared with adenocarcinoma, even when the size of the mass is large. MR features of lymphoma include homogeneous intermediate T1 signal and increased T2 signal (Fig. 7) [6]. Mild to moderate enhancement is seen after the administration of gadolinium. Lymphoma demonstrates marked diffusion restriction with a lower apparent diffusion coefficient (ADC) than other tumors due to high cellularity and high nucleus to cytoplasm ratio [23].

Metastasis

Metastasis is in the differential diagnosis of rectal wall tumors. Imaging features are variable and may or may not follow imaging characteristics of the primary tumor. Figure 8 illustrates a case of metastatic lobular breast cancer to the rectal wall. The patient had a remote history of lobular breast cancer with clinical presentation mimicking rectal carcinoma. Key features on MRI in this example are the infiltrative nature of the tumor in the rectal wall and the bladder.

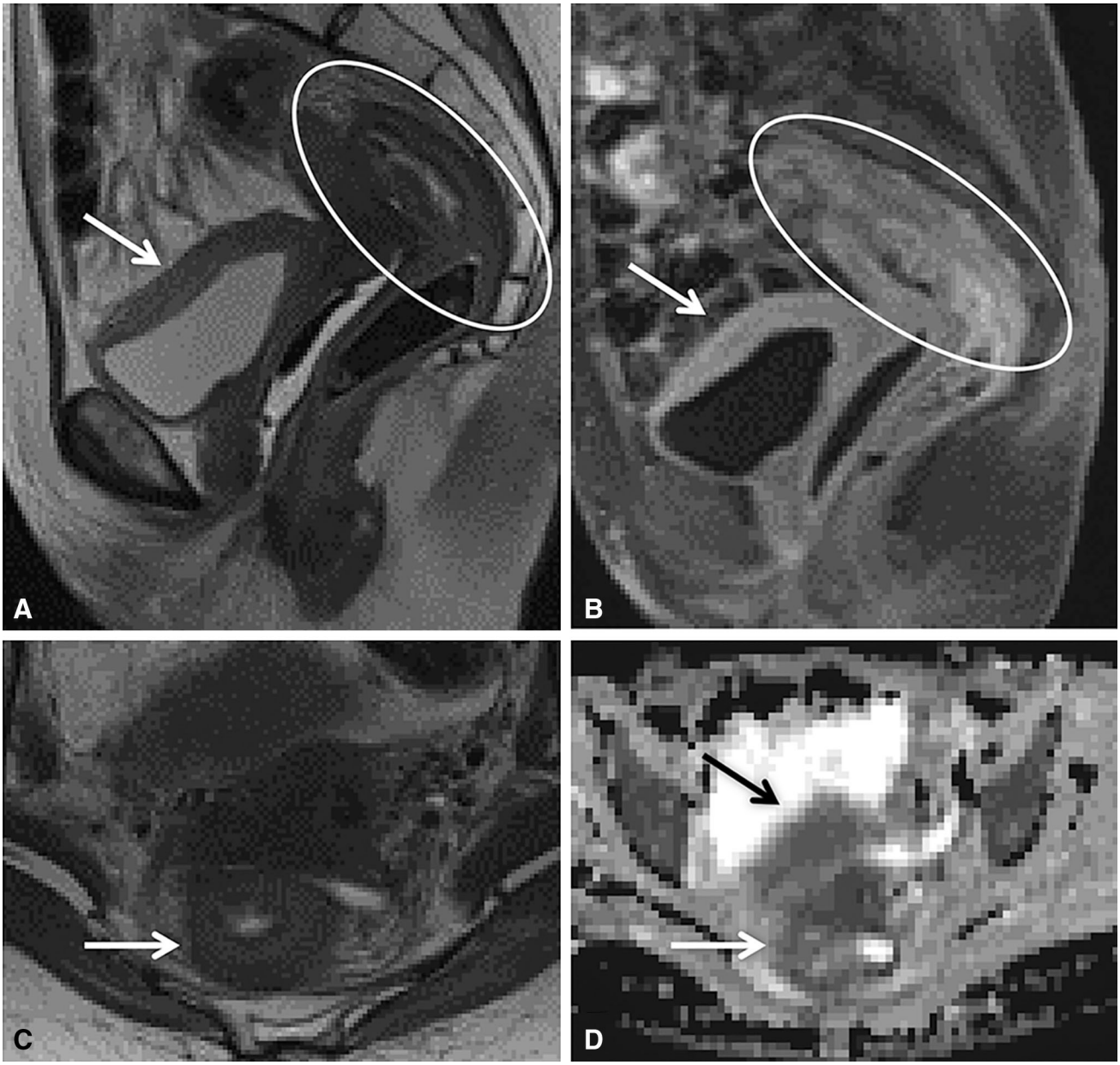

Fig. 8. Biopsy proven lobular breast cancer metastasis. **A** Sagittal T2-weighted image shows wall thickening with infiltrative tumor in the rectum (circled) and involving the bladder dome (arrow). **B** Sagittal post-contrast T1-weighted image demonstrates avid tumor enhancement along the bladder dome (arrow) and rectum (circled). **C** Axial T2-weighted image shows circumferential wall thickening by the tumor (arrow). **D** Apparent diffusion coefficient map shows low ADC of the tumor involving the bladder (black arrow) and rectum (white arrow).

Melanoma

Primary anorectal melanoma is rare, comprising 1% of all anorectal malignancy [24]. However, melanoma can metastasize anywhere in the body and hematogenous spread of disease can result in mural deposits of tumor in the rectal wall [25]. Melanin is paramagnetic with high T1 signal as a distinguishing feature; however, approximately 10%–29% of anorectal melanoma is amelanotic

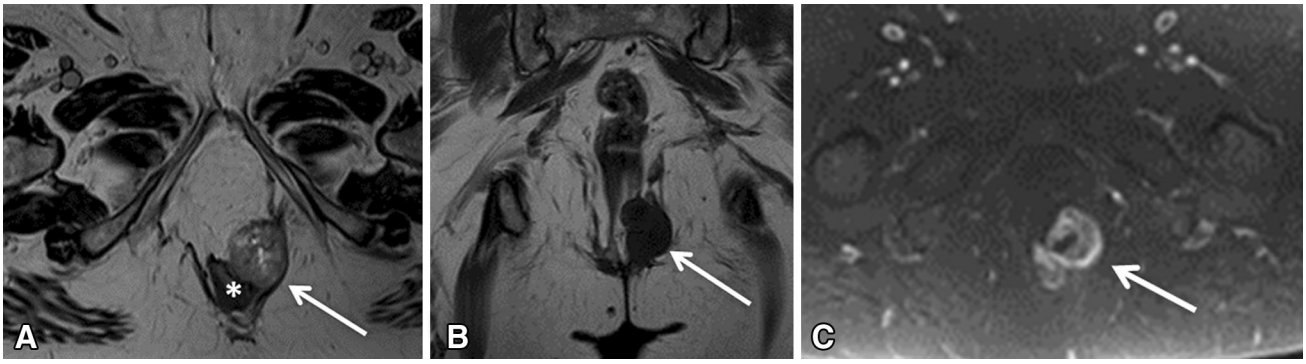

Fig. 9. Biopsy proven melanoma metastasis to the perirectal region. Patient had a history of vaginal melanoma with pelvic floor reconstruction. **A** Axial small field of view T2-weighted image demonstrates a mixed T2 signal mass displacing the rectum (asterisk) towards the right and the pelvic floor myocutaneous flap to the left (arrow). **B** On coronal T1 weighted image, the mass was amelanotic and demonstrates low T1 signal (arrow). **C** Post-contrast axial T1-weighted image shows avid enhancement (arrow).

and will resemble rectal adenocarcinoma on MRI [26]. T2 signal is mixed and there may be hemorrhage within the mass. Melanoma metastases demonstrate avid enhancement on post-contrast imaging (Fig. 9).

Myofibroblastic sarcoma

Myofibroblastic sarcoma is a very rare malignant soft tissue tumor composed predominantly of differentiated myofibroblasts [27]. There are only a few reported cases in the literature, and to our knowledge, none are of rectal origin. Figure 10 shows a case of a rectal myofibroblastic sarcoma in an 80-year-old man with a history of prostate cancer treated with radiation therapy. One and a half years after treatment he was found to have high-grade myofibroblastic sarcoma of the rectum. In this case, axial T2-weighted MRI shows a polypoid lesion arising from the anterior rectal wall, with associated enhancement and diffusion restriction.

Colitis cystica profunda

Colitis cystica profunda can be found anywhere along the gastrointestinal tract, but is most commonly described in the colon. It is an uncommon benign condition characterized by mucin-filled cysts located in the submucosa, frequently associated with solitary ulcer and rectal prolapse syndromes [28]. The etiology remains unclear, but inflammation, mucosal trauma, and rectal prolapse have been suggested. Additional reported associations include ulcerative colitis, Crohn's disease, adenomatous polyps, Peutz–Jegher syndrome, and spastic colitis [29]. This entity may occur at any age, but is most common in the third and fourth decades [30]. Patients may be asymptomatic or present with symptoms mimicking rectal malignancy, such as rectal bleeding, tenesmus, and diarrhea.

Described features on transrectal ultrasound include multiple cysts of varying sizes in the rectal submucosa, with few internal echoes, and absence of penetration beyond the submucosa [30]. There is a paucity of information in the literature regarding MRI features. However, in a case published by Inan et al. [28], the appearance was that of multiple circumscribed submucosal cysts, which were homogeneously hyperintense on T2-weighted (Fig. 11) and hypointense on T1-weighted images. On contrast-enhanced sequences, no significant contrast enhancement was detected. Treatment can be medical or surgical according to the severity of symptoms.

Perirectal/presacral space

A variety of masses, benign and malignant, can arise from the tissue elements in the mesorectum and presacral space. Contents in this location include osteochondral tissue, neural tissue and soft tissues of the pelvis [11]. Knowledge of specific imaging features can assist in the differential diagnosis. Pathology from adjacent organs in the pelvis can also involve the rectum and potentially simulate a rectal mass. The superior soft tissue contrast of MRI aids in determining the origin of a perirectal mass.

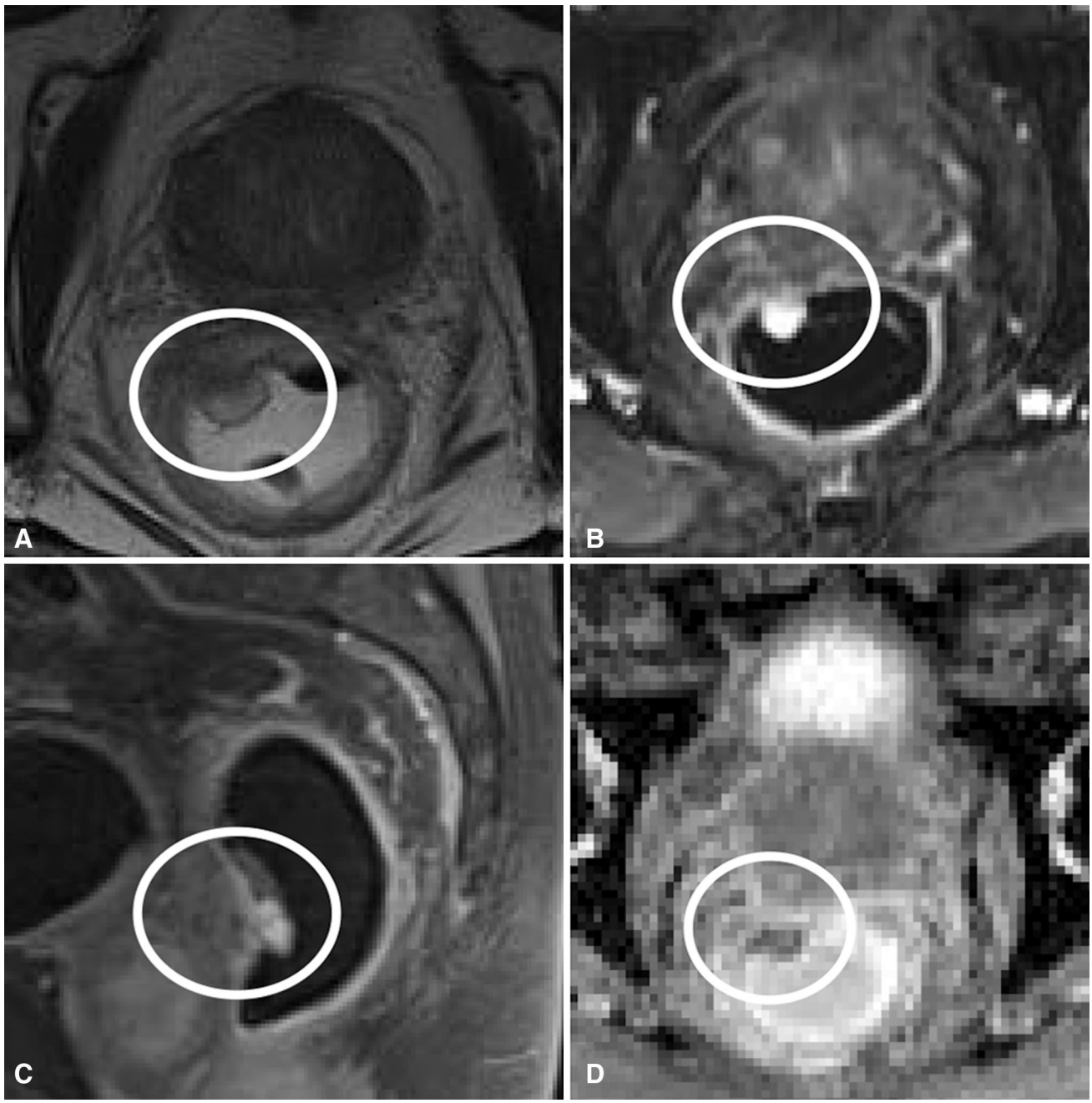

Fig. 10. Surgically proven rectal myofibroblastic sarcoma. **A** Axial T2-weighted MRI with rectal gel shows an intermediate T2 signal polypoid lesion (circled) arising from the right anterior rectal wall. This lesion shows enhancement on **B** axial and **C** sagittal post-contrast images, with restricted diffusion on **D** ADC map.

Developmental cysts

Developmental cysts are the most common congenital entity encountered in the presacral space [31]. They are defined as benign epithelial cysts that are thought to arise from caudal embryonic vestiges [5]. These cysts can be classified as enteric, epidermoid, dermoid, or neurenteric according to the tissue origin and histopathologic features. Developmental cysts are often asymptomatic, but may present with symptoms due to local mass effect such as constipation, rectal fullness, and pelvic pain.

A well-defined, unilocular or multilocular, thin-walled cystic lesion is the main imaging feature [31]. They usually affect middle age women and are often incidentally detected. Complications include rectal bleeding, infection, and recurrent perianal fistulas. In some cases, surgical excision is necessary to confirm diagnosis and prevent complications. Rare malignant transformation to adenocarcinoma, carcinoid, or squamous carcinoma has been reported [5, 31].

Enteric and neurenteric cysts

Enteric cysts are partially or completely lined with intestinal mucosa [31]. There are two types of enteric cysts: the more common tailgut cyst (also known as retrorectal cyst-hamartoma [RRCH] or mucin-secreting cyst) and the more rare rectal duplication cyst (comprises 5% of all duplication cysts) [5]. The tailgut cyst is lined by an assortment of enteric mucosa and lacks a muscle coat; in contrast to the duplication cyst which contains a muscle coat, is lined by rectal mucosa (in addition to possible ectopic mucosa), and is in continuity with the rectum [4]. Neurenteric cysts differ in that they are lined by a mature mucosa of endodermal origin, for instance bladder, and contain a lamina propria [4].

The tailgut is the most caudal part of the hindgut, distal to the future anus. Normally, it involutes by the eighth week of embryonic development, but if a remnant persists, it may give rise to a tailgut cyst [32]. Tailgut cysts are the most common incidentally found presacral lesion in adults [11]. A tailgut cyst may adhere to the sacrum or rectum, but it does not invade the sacrum or communicate with the rectal lumen [6, 31]. CT shows a well-marginated low attenuation lesion with no enhancement. On MRI, tailgut cysts show variable T1- and T2-weighted signal intensity depending on the internal contents, but are often low signal intensity on T1-weighted and high signal intensity on T2-weighted images (Fig. 12). It has been reported that a multilocular appearance with internal septa on T2-weighted images is a finding unique to tailgut cysts [33].

Epidermoid and dermoid cysts

Epidermoid and dermoid cysts are benign lesions lined with stratified squamous epithelium [31]. Dermoid cysts differ in that they contain skin appendages (ex, hair follicles and sweat glands) and may contain a fatty fluid content rather than the clear fluid of an epidermoid [3]. In contrast to the RRCH which is usually multiloculated, this type of cyst is frequently unilocular. Similar to RRCH, epidermoid and dermoid cysts show a well-defined, thin-walled cyst on MRI that is commonly low signal on T1-weighted images and high signal on T2-weighted images, although the signal can vary depending on cyst contents (Fig. 13).

Focal irregular wall thickening with enhancement in any of the developmental cysts is suggestive of malignant degeneration. Wall thickening with surrounding inflam-

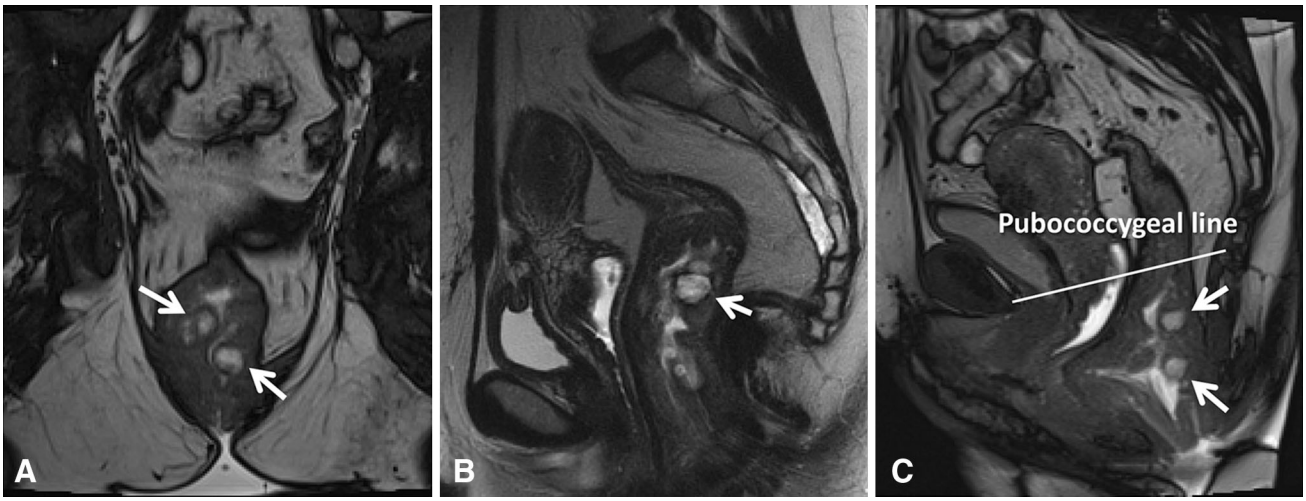

Fig. 11. Colitis cystica profunda. **A** Coronal and sagittal **B** images from dynamic fast imaging with steady-state precession (FISP) show multiple hyperintense submucosal cysts (small arrows). **C** Sagittal FISP image obtained at maximum strain shows evidence of rectal prolapse, anterior rectocele and mucosal redundancy. Rectal and vaginal gel was instilled on this pelvic floor exam.


A
B
C
D
E
F
G

◀**Fig. 12.** Surgically proven retrorectal cystic hamartoma or tailgut cyst. **A** Axial and **B** sagittal unenhanced CT images show a homogeneously hypodense mass (circled) in the presacral space. **C** T2-weighted axial and **D** sagittal MR images better characterize this lesion (circled) as a T2 hyperintense, multilocular cystic lesion that displaces the rectum (asterisk) anteriorly. **E** No signal loss on T2-weighted fat-sat images (circled). **F** Pre-contrast T1-weighted image demonstrates T1 hyperintensity in a cystic locule (circled), suggesting mucoid, proteinaceous, or hemorrhagic content. **G** No evidence of enhancement on post-contrast imaging (circled).

mation is suggestive of superinfection [31]. Clinical history is helpful in distinguishing between the two.

Presacral extramedullary hematopoiesis

It is thought that extramedullary hematopoiesis is a physiologic compensatory phenomenon in the setting of congenital hemoglobinopathies or acquired marrow replacement disorders [34]. It most commonly involves the spleen and liver, and occasionally lymph nodes, as these are hematopoietic organs during embryonic life. Paravertebral and presacral sites are uncommon.

CT shows a heterogeneous lobulated soft tissue density mass, sometimes with macroscopic fat (Fig. 14). Intralesional fat can be confirmed on MRI as high signal on T1- and T2-weighted images with evidence of signal drop out on fat suppressed images. Increased lesion activity on radionuclide bone marrow imaging supports the diagnosis. Surgery is only considered in symptomatic patients [35]. Chemotherapy for underlying myeloproliferative disorder or radiation to reduce the volume of the mass are treatment considerations.

Gynecologic pathology

Gynecologic processes can involve the rectum due to their close anatomic relationship.

Ovarian pathology

Solid and cystic ovarian neoplasms could potentially be misinterpreted as a primary rectal/perirectal lesion (Fig. 15). Key imaging findings for the correct diagnosis include identification of the ovarian origin and demonstration of a clear separation from the adjacent rectal wall.

Endometriosis

Deep pelvic endometriosis is defined as subperitoneal invasion of endometrial implants. Commonly involved areas include the posterior-cul-de-sac, uterosacral ligaments, rectum, rectovaginal septum, vagina, and bladder [36]. The rectosigmoid is the segment of bowel most commonly involved [37]. Implants are usually serosal, but can invade deeper with subsequent thickening and fibrosis of the muscularis propria [37]. Adhesions and gastrointestinal obstruction may develop.

On MRI, involvement of adjacent structures, including the rectum, should be suspected when there is a hypointense thickened or nodular appearance on T2-weighted images [37]. These areas may or may not demonstrate foci of T2 hyperintense signal, corresponding to dilated ectopic endometrial glands and foci of T1 hyperintense signal representing regions of hemorrhage (Fig. 16). Enhancement is variable, depending on the extent of inflammatory reaction, glandular tissue, and fibrosis.

Multicystic benign mesothelioma

Mesothelial tumors of the peritoneum include benign adenomatoid tumors, malignant mesothelioma, and cystic mesothelioma (multicystic benign mesothelioma) [38]. The latter is an intermediate-grade neoplasm of the mesothelial cells of the peritoneum [39]. As the name implies, it is a multicystic diffuse lesion involving the peritoneum, omentum, and pelvic abdominal viscera [38]. It is most often seen in women of childbearing age. Cysts are commonly found at sites of prior surgery or pelvic inflammatory disease [36], and they tend to recur locally. A possible hormonal sensitivity has been suggested since it is most often found in women of childbearing age, and a decrease in cyst size has been shown after treatment with gonadotropin-releasing hormone analog agonist and tamoxifen [40].

On CT and MRI, a thin-walled multicystic mass with non-calcified septa is seen (Fig. 17). Imaging findings that help in its differentiation include: cysts with smooth borders that insinuate around adjacent structures, no adenopathy, no scalloping of the liver and spleen (as seen in pseudomyxoma peritonei), and no peritoneal or

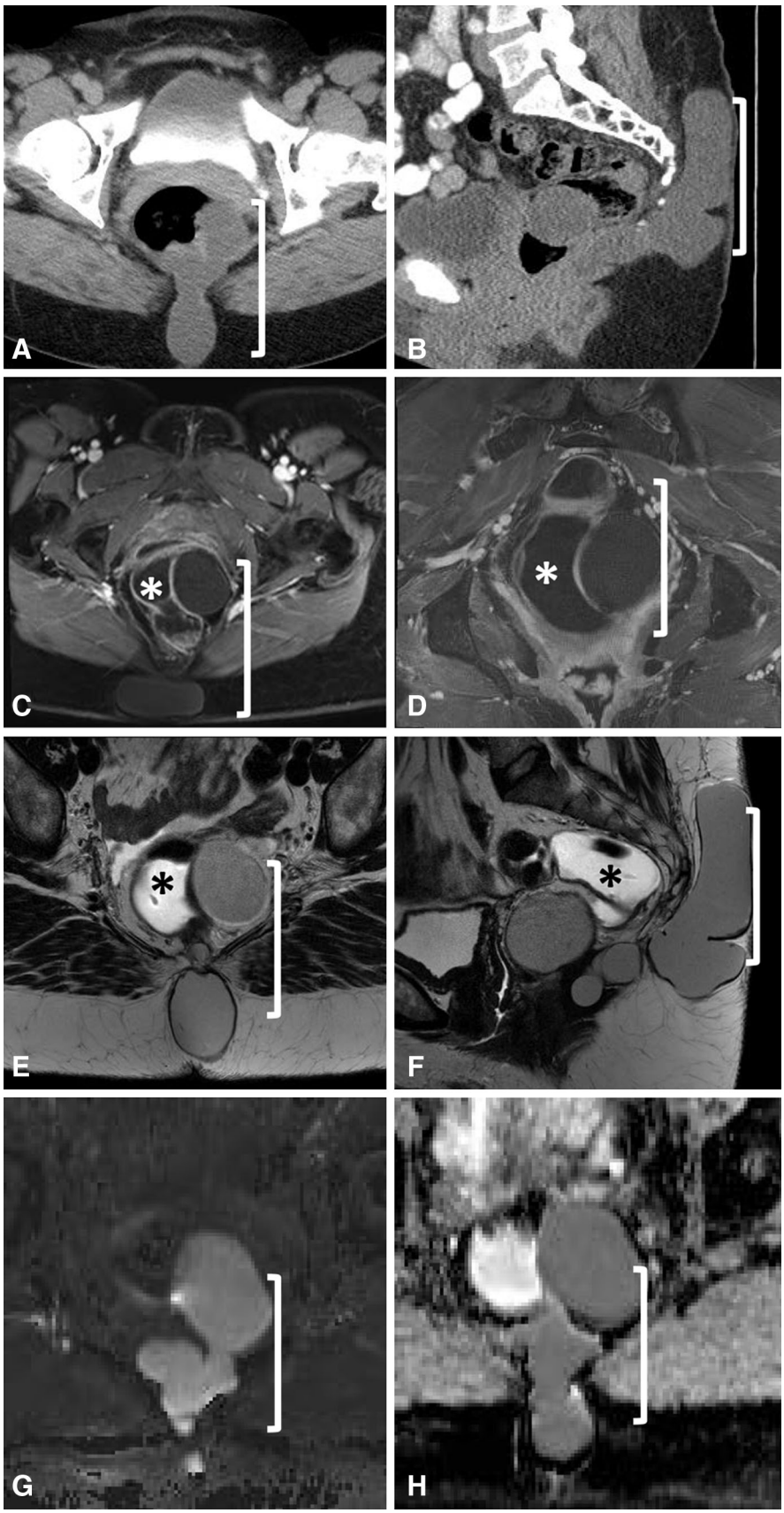

Fig. 13. Surgically proven epidermoid cyst. **A** Axial CECT shows a non-enhancing perirectal cystic lesion (bracketed). **B** Sagittal CECT demonstrates posterior subcutaneous extension of this lesion. **C** Axial and **D** coronal fat-sat T1-weighted post-contrast MRI shows a non-enhancing low T1 signal lesion. The mass results in compression of the gel-filled rectum (asterisk). This lobular but unilocular lesion shows intermediate signal on **E** axial and **F** sagittal T2-weighted images. Minimal restricted diffusion on **G** high B value and **H** ADC images.

Fig. 14. Presacral extramedullary hematopoiesis. **A** Sagittal T2-weighted image shows two smooth lobulated presacral lesions (circled) with evidence of intralesional fat (arrow). **B** Sagittal T1-weighted fat-saturated post-contrast image confirms intralesional fat component (arrow) and homogeneous soft tissue enhancement. **C** Macroscopic fat (arrow) is also evident on axial CT.

omental implants (as expected with peritoneal carcinomatosis). Complete surgical excision is the treatment of choice.

Metastases

Metastatic disease has a variable appearance depending on the tumor of origin. Metastatic disease of the perirectal region can occur from direct invasion along the peritoneal reflections, intraperitoneal seeding in the pelvis from ascitic fluid, embolic hematogenous spread, and lymphatic extension [25].

Sacrum

The sacrum forms the posterior border of the pelvis and mass lesions originating from the sacrum can be difficult to separate from the rectum. It is important to assess involvement of the sacrum when evaluating presacral masses. Osteochondral and neurogenic tumors typically remodel or destroy the sacrum [41].

Sacrococcygeal teratoma

Sacrococcygeal teratoma is a germ cell tumor containing elements derived from all three germ layers. They arise from cells within the anterior portion of the coccyx [42]. It is the most common presacral tumor in children [11]. Less than 10% are diagnosed in patients > 2 years old, the majority of which are located internally in the abdomen or pelvis and more likely to be malignant [11].

Imaging features depend on internal contents. Benign teratomas contain only mature tissues (i.e., fluid, fat, calcification) and are predominantly cystic (Fig. 18). Malignant tumors have more solid components with areas of hemorrhage and necrosis. At surgery, the coccyx is resected with the tumor to reduce rate of recurrence.

Sacral chordoma

Chordoma is the most common primary malignant tumor of the sacrum, typically involving the fourth and fifth sacral vertebrae [5]. It arises from the notochord remnants and usually lies in a midline or paramedian location. This lesion affects individuals in a broad age distribution (fourth to seventh decade) with a male-to-female ratio of 2–3:1 [43]. The most common presenting symptom is pain in the lower back or sciatic region, followed by constipation, neurologic compromise, and a sacral or gluteal mass [44].

CT can be very helpful for defining the extent of bone involvement. Bone destruction with an associated lobulated midline soft tissue mass is typical [43]. The mass can show areas of low attenuation reflecting the myxoid properties, as well as punctate areas of higher attenuation representing calcifications. At MRI, the most striking feature of chordoma is the markedly high signal intensity on T2-weighted images (Fig. 19) [43]. They are predominantly hypointense

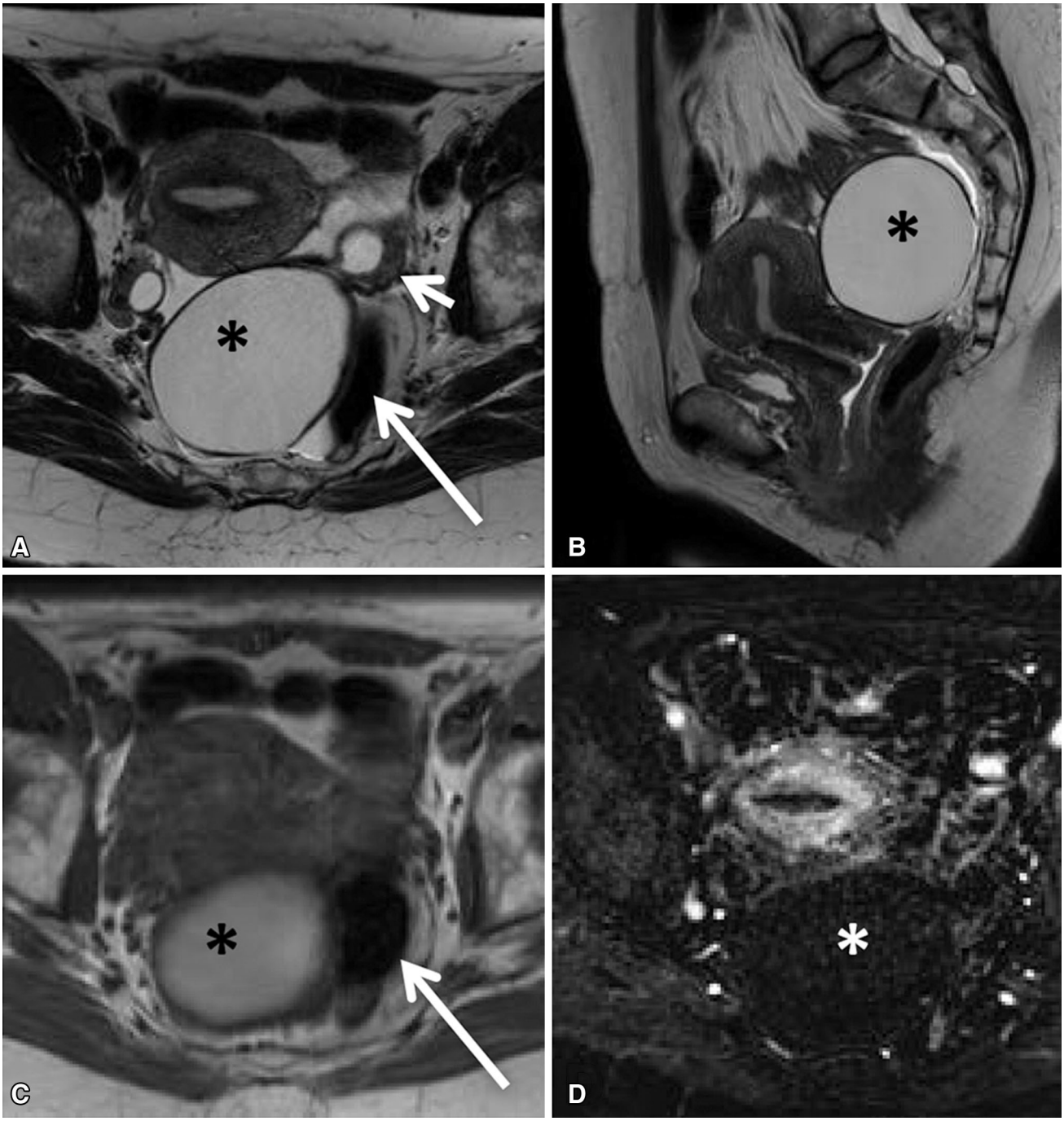

Fig. 15. Surgically proven ovarian papillary serous cystadenofibroma. **A** Axial and **B** sagittal T2-weighted images show a hyperintense cystic lesion (asterisk) arising from the left ovary (short arrow). The lesion displaces the rectum laterally (long arrow). **C** Pre-contrast T1-weighted image shows intrinsic T1 hyperintense signal in the cystic lesion (asterisk). The rectum is displaced towards the left (arrow). **D** Post-contrast subtraction image reveals no enhancement (asterisk).

or isointense to muscle on T1-weighted images. Occasionally, areas of intrinsic T1 hyperintense signal representing hemorrhage or mucinous material can be seen.

Chordomas are generally considered slow-growing lesions, but are locally aggressive. They require radical en bloc resection with wide margins to affect a cure [44, 45].

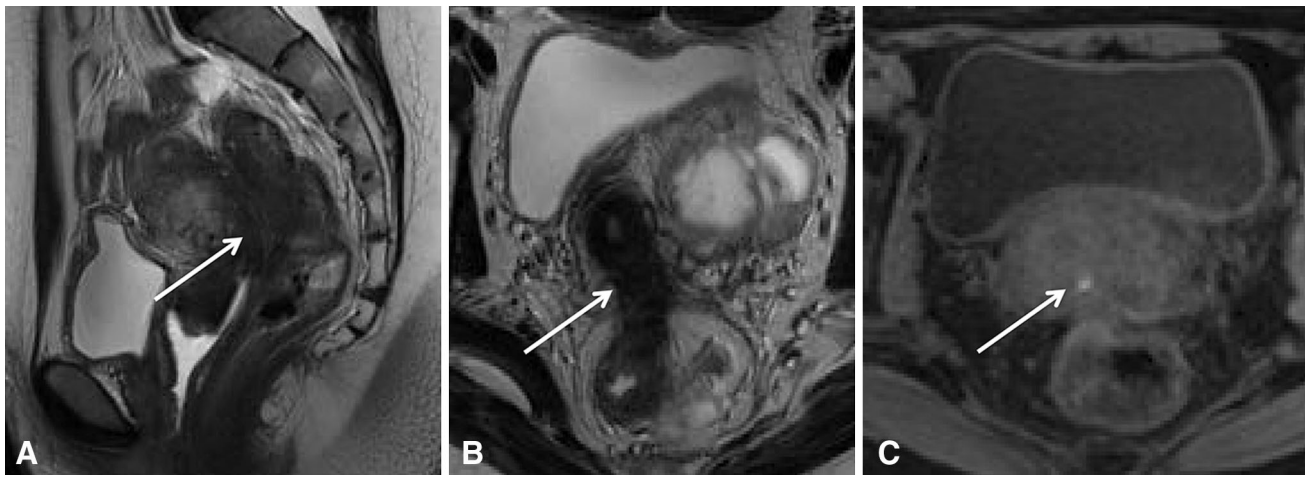

Fig. 16. Biopsy proven invasive endometriosis. **A** Sagittal T2-weighted image shows extensive fibrosis (arrow), which obliterates the rectovaginal septum and invades the anterior rectal wall. **B** Axial T2-weighted and **C** fat-saturated T1-weighted images show T2 hypointense fibrosis with associated T1 hyperintense foci (arrowhead) consistent with hemorrhage.

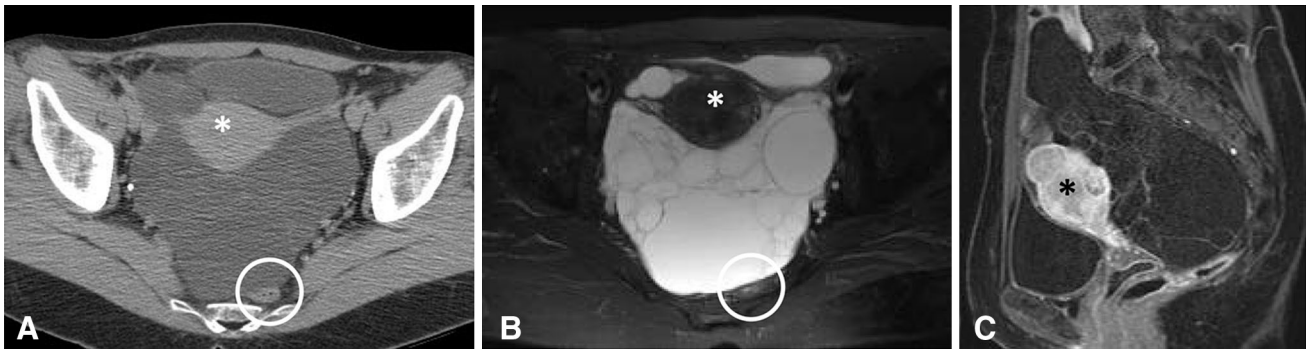

Fig. 17. Surgically proven multicystic benign mesothelioma. **A** Axial CECT shows a large cystic mass which compresses the rectum (circled) posteriorly. **B** Axial T2-weighted image demonstrates the multicystic nature of this mass and better defines multiple thin septations. **C** Sagittal post-contrast T1-weighted fat-saturated image shows no suspicious enhancement. Incidental fibroid uterus (asterisk).

The use of radiation and chemotherapy for this type of tumor is debatable. Antitumoral activity of monoclonal antibodies may provide improved outcomes for poor surgical candidates and recurrent tumors.

Neurogenic masses

Schwannomas and neurofibromas in the presacral region arise from the lower lumbar and sacral dorsal sensory nerve roots. They are rare, generally benign tumors, but can become very large in size. Neurofibromas have potential for malignant degeneration. Solitary neurofibroma can be indistinguishable from schwannoma based on imaging alone. The presence of multiple nerve sheath tumors suggests neurofibromatosis [41].

Schwannoma

Presacral schwannoma is often large and there may be associated remodeling or erosion of the sacrum. Calcifications may or may not be present. Schwannoma is heterogeneous in appearance on MR with low T1 signal

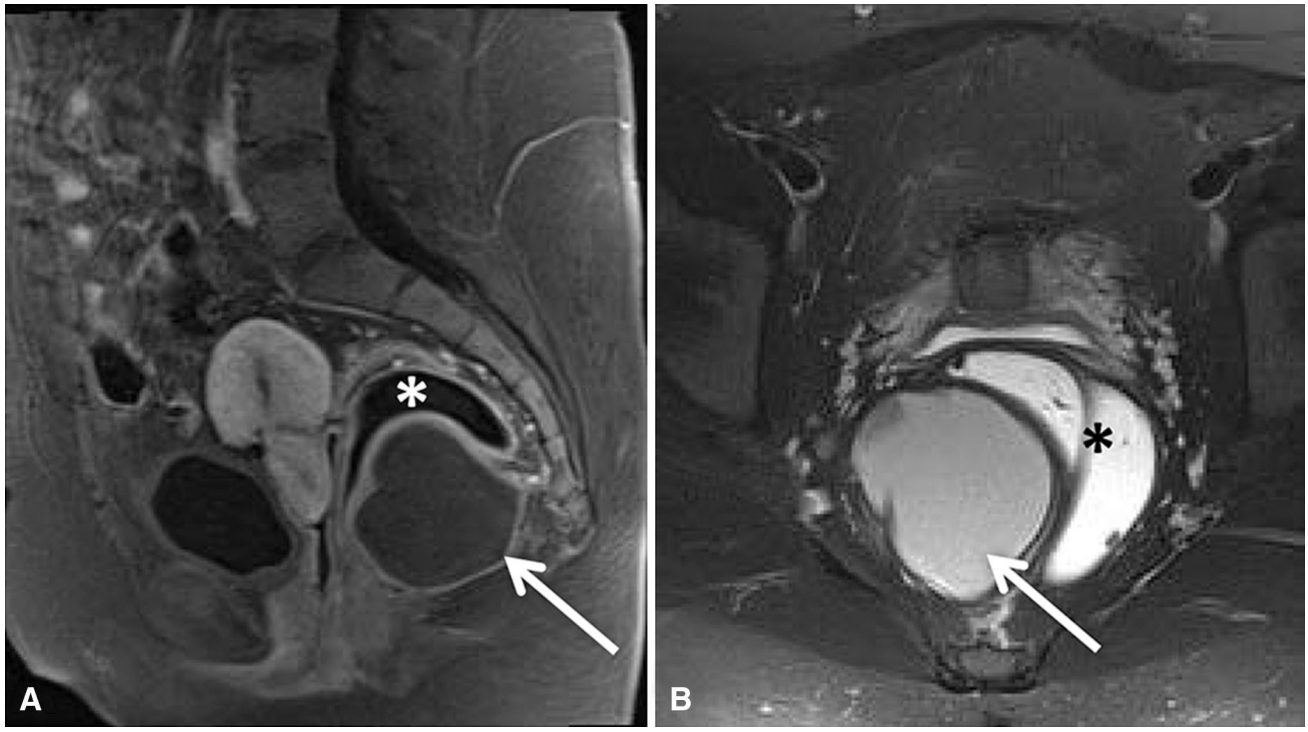

Fig. 18. Surgically proven mature sacrococcygeal teratoma. **A** Sagittal post-contrast image shows a non-enhancing well-demarcated cystic lesion (arrow) exerting mass effect on the adjacent rectum (asterisk) which contains gel. **B** Axial fat-saturated T2-weighted image shows internal intermediate T2 signal without focal nodularity or solid component.

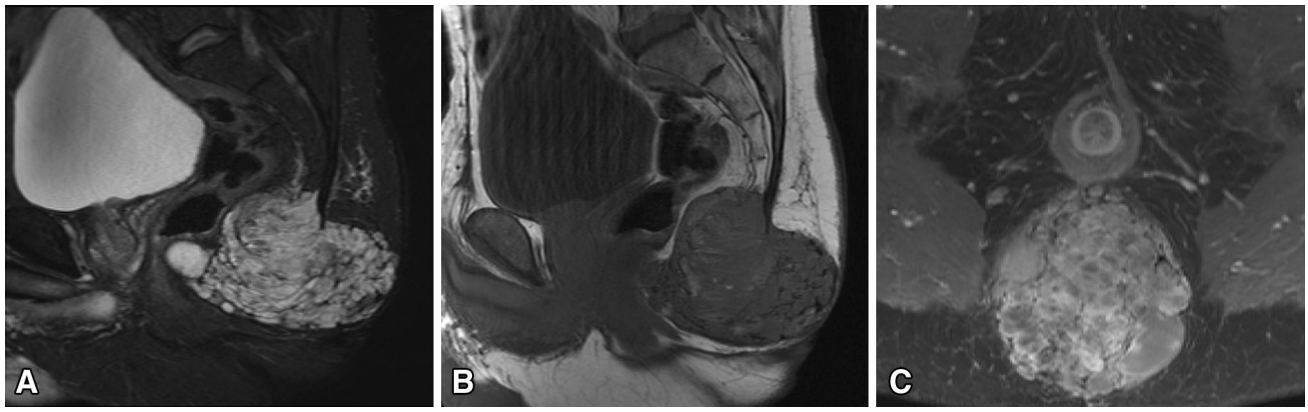

Fig. 19. Surgically proven sacral chordoma. **A** Sagittal fat-saturated T2-weighted image shows a hyperintense mass centered midline in the distal sacrum. **B** Sagittal T1-weighted image shows a predominantly hypointense mass with several hyperintense foci, suggesting hemorrhagic or mucinous material. Abnormal marrow signal and loss of definition of the distal sacral segments are suggestive of the underlying osseous origin. **C** Axial post-contrast fat-saturated image shows heterogeneous enhancement.

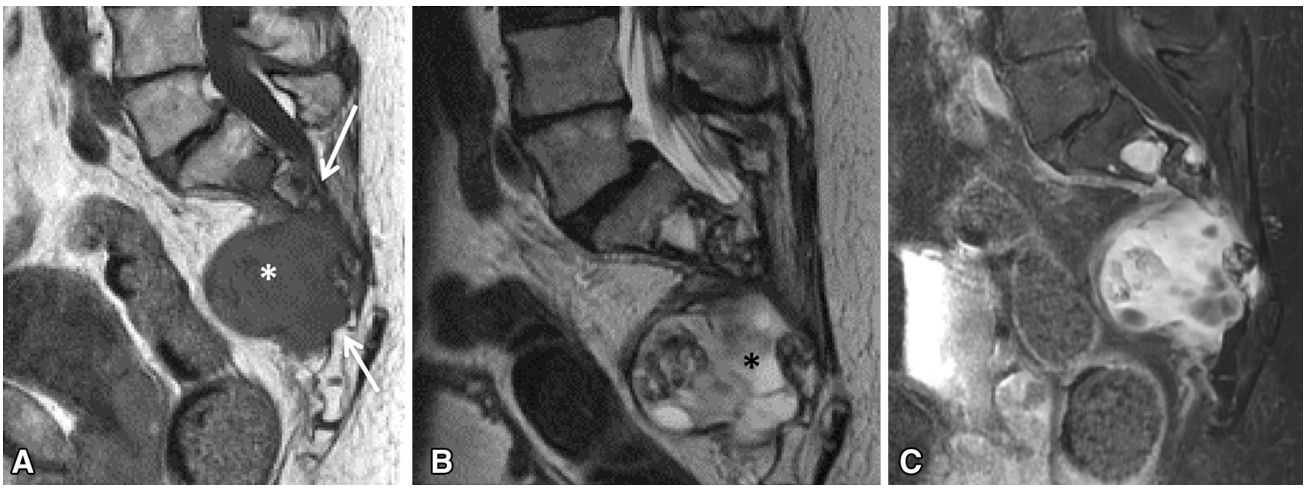

Fig. 20. Biopsy proven sacral schwannoma. **A** Sagittal T1-weighted image demonstrates a low T1 signal intensity mass (asterisk) in the presacral space with erosion and remodeling of the sacrum (arrows). **B** Sagittal T2-weighted image shows heterogeneous predominantly high T2 signal intensity in the mass (asterisk). **C** Sagittal fat suppressed T1-weighted image after the administration of gadolinium contrast illustrates avid heterogeneous enhancement.

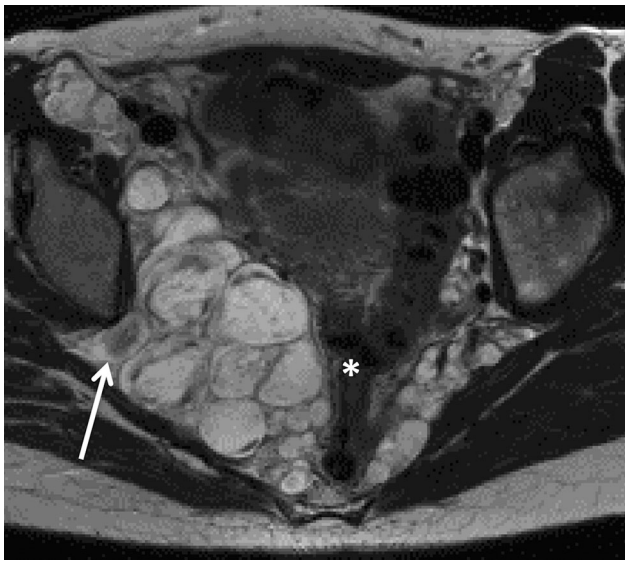

Fig. 21. Plexiform neurofibroma. Axial T2-weighted image demonstrates large plexiform neurofibromas in the pelvis with mass effect on the rectum (asterisk). Note the high T2 signal intensity with the target sign (arrow) due to a central low signal intensity fibrous core.

intensity and high T2 signal intensity (Fig. 20). Schwannomas tend to have a thin pseudocapsule and small internal cystic change [11].

Neurofibroma

Neurofibromas are homogenous on T1-weighted images with iso- to mildly hyperintense signal relative to skeletal muscle. A target appearance on T2-weighted images is a characteristic feature of neurofibroma and is due to a central low signal fibrous core with a hyperintense rim of myxoid material (Fig. 21) [11].

Anterior meningocele

Anterior meningocele is a cerebrospinal fluid (CSF) containing sac that herniates anteriorly through a sacral foramen or sacral defect and may be associated with partial sacral agenesis. Anterior meningoceles are less common than posterior meningoceles, but 80% manifest in the first decade of life [11]. They may be present as asymptomatic or symptomatic pelvic masses, can be quite large, and may be confounded with other

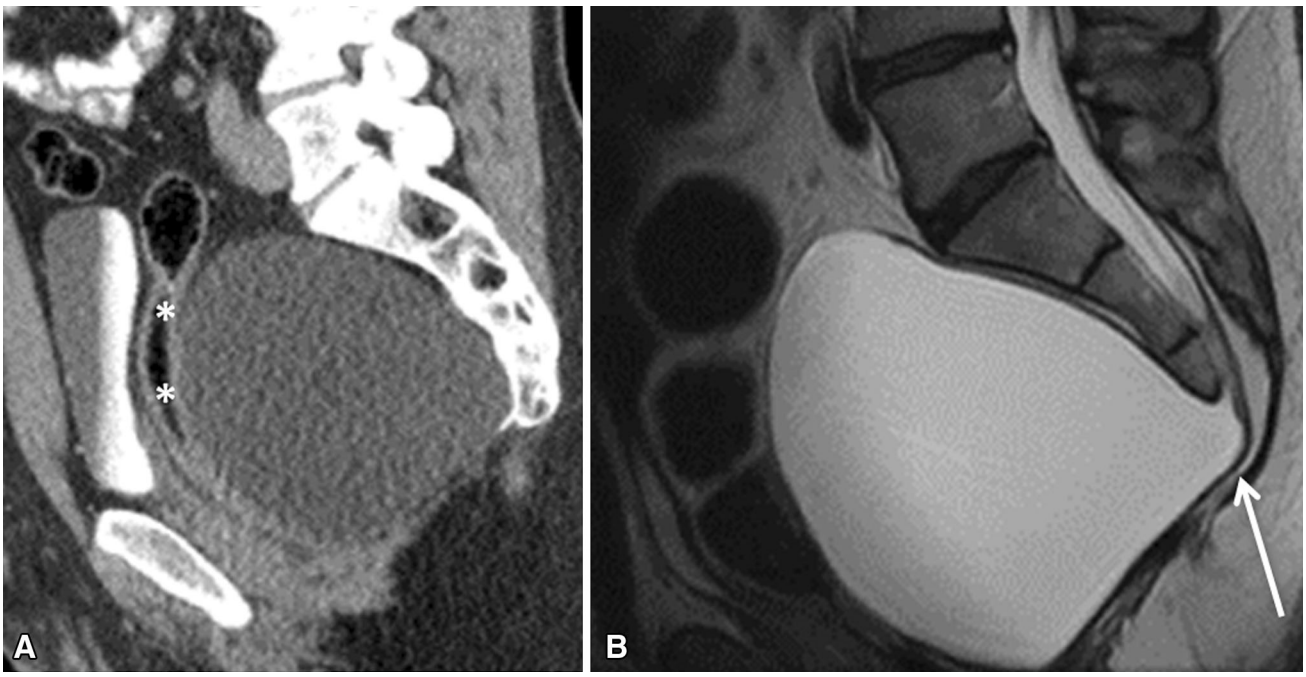

Fig. 22. Anterior sacral meningocele. **A** CT demonstrates a large presacral cystic mass which contacts and displaces the rectum anteriorly (asterisks). **B** Sagittal T2-weighted MRI demonstrates spinal dysraphism with partial sacral agenesis and large anterior herniation of a sacral meningocele (arrow).

cysts in the pelvis [41]. Symptoms are most commonly related to pressure on the adjacent pelvic organs and nerve roots and include dysmenorrhea, constipation, and urinary incontinence [11]. Surgical excision is generally performed as the risk of complication increases with time.

Osseous features associated with meningocele are better assessed on CT and include vertebral body scalloping, hypoplasia, and aplasia. Otherwise, MR is the optimal modality for evaluating meningocele (Fig. 22). MR demonstrates a large cystic mass that follows CSF signal intensity on all sequences. MR can assess neural elements in the meningocele and best depicts any sacral defects or dysraphism [11, 41].

Conclusion

Clinical presentation of rectal and perirectal diseases is often misleading and not necessarily related to rectal adenocarcinoma. Radiologists need to be aware of uncommon pathologies in this region in order to facilitate optimal management decisions.

Compliance with ethical standards

Funding Not applicable.

Conflict of interest None. All authors declare no conflict of interest.

Ethical approval This article does not contain any studies with human participants or animals performed by any of the authors.

References

1. Kenig J, Richter P (2013) Definition of the rectum and level of the peritoneal reflection—still a matter of debate? Wideochir Inne Tech Maloinwazyjne 8:183–186. https://doi.org/10.5114/wiitm.2011.34205
2. Iafrate F, Laghi A, Paolantonio P, et al. (2006) Preoperative staging of rectal cancer with MR imaging: correlation with surgical and histopathologic findings. Radiographics 26:701–714. https://doi.org/10.1148/rg.263055086
3. Levy AD, Remotti HE, Thompson WM, Sobin LH, Miettinen M (2003) Anorectal gastrointestinal stromal tumors: CT and MR imaging features with clinical and pathologic correlation. AJR Am J Roentgenol 180:1607–1612. https://doi.org/10.2214/ajr.180.6.1801607
4. Levy AD, Remotti HE, Thompson WM, Sobin LH, Miettinen M (2003) Gastrointestinal stromal tumors: radiologic features with pathologic correlation. Radiographics 23:283–304 (quiz 532). https://doi.org/10.1148/rg.232025146
5. Rouse HC, Godoy MC, Lee WK, et al. (2008) Imaging findings of unusual anorectal and perirectal pathology: a multi-modality approach. Clin Radiol 63:1350–1360. https://doi.org/10.1016/j.crad.2008.06.008
6. Kim H, Kim JH, Lim JS, et al. (2011) MRI findings of rectal submucosal tumors. Korean J Radiol 12:487–498. https://doi.org/10.3348/kjr.2011.12.4.487
7. Hong X, Choi H, Loyer EM, et al. (2006) Gastrointestinal stromal tumor: role of CT in diagnosis and in response evaluation and surveillance after treatment with imatinib. Radiographics 26:481–495. https://doi.org/10.1148/rg.262055097
8. Franquemont DW (1995) Differentiation and risk assessment of gastrointestinal stromal tumors. Am J Clin Pathol 103:41–47
9. Fletcher CD, Berman JJ, Corless C, et al. (2002) Diagnosis of gastrointestinal stromal tumors: a consensus approach. Hum Pathol 33:459–465
10. Suster S (1996) Gastrointestinal stromal tumors. Semin Diagn Pathol 13:297–313
11. Hain KS, Pickhardt PJ, Lubner MG, Menias CO, Bhalla S (2013) Presacral masses: multimodality imaging of a multidisciplinary space. Radiographics 33:1145–1167. https://doi.org/10.1148/rg.334115171

12. Jiang ZX, Zhang SJ, Peng WJ, Yu BH (2013) Rectal gastrointestinal stromal tumors: imaging features with clinical and pathological correlation. World J Gastroenterol 19:3108–3116. https://doi.org/10.3748/wjg.v19.i20.3108
13. Pickhardt PJ, Kim DH, Menias CO, et al. (2007) Evaluation of submucosal lesions of the large intestine: part 1. Neoplasms. Radiographics 27:1681–1692. https://doi.org/10.1148/rg.276075027
14. Jacob AG, Driscoll DJ, Shaughnessy WJ, et al. (1998) Klippel–Trenaunay syndrome: spectrum and management. Mayo Clin Proc 73:28–36. https://doi.org/10.1016/S0025-6196(11)63615-X
15. Cha SH, Romeo MA, Neutze JA (2005) Visceral manifestations of Klippel–Trenaunay syndrome. Radiographics 25:1694–1697. https://doi.org/10.1148/rg.256055042
16. Servelle M, Bastin R, Loygue J, et al. (1976) Hematuria and rectal bleeding in the child with Klippel and Trenaunay syndrome. Ann Surg 183:418–428
17. Wilson CL, Song LM, Chua H, et al. (2001) Bleeding from cavernous angiomatosis of the rectum in Klippel–Trenaunay syndrome: report of three cases and literature review. Am J Gastroenterol 96:2783–2788. https://doi.org/10.1111/j.1572-0241.2001.04110.x
18. Levy AD, Sobin LH (2007) From the archives of the AFIP: gastrointestinal carcinoids: imaging features with clinicopathologic comparison. Radiographics 27:237–257. https://doi.org/10.1148/rg.271065169
19. Wong WL, Johns TA, Herlihy WG, Martin HL (2004) Best cases from the AFIP: multicystic mesothelioma. Radiographics 24:247–250. https://doi.org/10.1148/rg.241035068
20. Onaitis MW, Kirshbom PM, Hayward TZ, et al. (2000) Gastrointestinal carcinoids: characterization by site of origin and hormone production. Ann Surg 232:549–556
21. Jiang C, Gu L, Luo M, Xu Q, Zhou H (2015) Primary rectal lymphoma: a case report and literature review. Oncol Lett 10:43–44. https://doi.org/10.3892/ol.2015.3164
22. Ghai S, Pattison J, O'Malley ME, Khalili K, Stephens M (2007) Primary gastrointestinal lymphoma: spectrum of imaging findings with pathologic correlation. Radiographics 27:1371–1388. https://doi.org/10.1148/rg.275065151
23. Toledano-Massiah S, Luciani A, Itti E, et al. (2015) Whole-body diffusion-weighted imaging in Hodgkin lymphoma and diffuse large B-cell lymphoma. Radiographics 35:747–764. https://doi.org/10.1148/rg.2015140145
24. van Schaik PM, Ernst MF, Meijer HA, Bosscha K (2008) Melanoma of the rectum: a rare entity. World J Gastroenterol 14:1633–1635
25. Healy JC (2001) Detection of peritoneal metastases. Cancer Imaging 1:4–12. https://doi.org/10.1102/1470-7330.2001.002
26. Hoeffel CC, Azizi L, Mourra N, et al. (2006) MRI of rectal disorders. AJR Am J Roentgenol 187:W275–W284. https://doi.org/10.2214/AJR.05.0508
27. Montgomery E, Goldblum JR, Fisher C (2001) Myofibrosarcoma: a clinicopathologic study. Am J Surg Pathol 25:219–228
28. Inan N, Arslan AS, Akansel G, et al. (2007) Colitis cystica profunda: MRI appearance. Abdom Imaging 32:239–242. https://doi.org/10.1007/s00261-006-9048-5
29. Sunagawa H, Kinjyou T, Nagahama M, Nishimaki T, Nakayama T (2005) Enteritis cystica profunda presenting as ileoileal intussusception in a child: report of a case. Surg Today 35:164–167. https://doi.org/10.1007/s00595-004-2912-4
30. Hulsmans FJ, Tio TL, Reeders JW, Tytgat GN (1991) Transrectal US in the diagnosis of localized colitis cystica profunda. Radiology 181:201–203. https://doi.org/10.1148/radiology.181.1.1887033
31. Dahan H, Arrive L, Wendum D, et al. (2001) Retrorectal developmental cysts in adults: clinical and radiologic-histopathologic review, differential diagnosis, and treatment. Radiographics 21:575–584. https://doi.org/10.1148/radiographics.21.3.g01ma13575
32. Yang DM, Park CH, Jin W, et al. (2005) Tailgut cyst: MRI evaluation. AJR Am J Roentgenol 184:1519–1523. https://doi.org/10.2214/ajr.184.5.01841519
33. Kim MJ, Kim WH, Kim NK, et al. (1997) Tailgut cyst: multilocular cystic appearance on MRI. J Comput Assist Tomogr 21:731–732
34. Mesurolle B, Sayag E, Meingan P, et al. (1996) Retroperitoneal extramedullary hematopoiesis: sonographic, CT, and MR imaging appearance. AJR Am J Roentgenol 167:1139–1140. https://doi.org/10.2214/ajr.167.5.8911166
35. Sauer B, Buy X, Gangi A, Roy C (2007) Exceptional localization of extramedullary hematopoiesis: presacral and periureteral masses. Acta Radiol 48:246–248. https://doi.org/10.1080/02841850601128991
36. Del Frate C, Girometti R, Pittino M, et al. (2006) Deep retroperitoneal pelvic endometriosis: MR imaging appearance with laparoscopic correlation. Radiographics 26:1705–1718. https://doi.org/10.1148/rg.266065048
37. Coutinho A Jr, Bittencourt LK, Pires CE, et al. (2011) MR imaging in deep pelvic endometriosis: a pictorial essay. Radiographics 31:549–567. https://doi.org/10.1148/rg.312105144
38. O'Neil JD, Ros PR, Storm BL, Buck JL, Wilkinson EJ (1989) Cystic mesothelioma of the peritoneum. Radiology 170:333–337. https://doi.org/10.1148/radiology.170.2.2643136
39. Koo PJ, Wills JS (2009) Case 146: benign multicystic mesothelioma. Radiology 251:944–946. https://doi.org/10.1148/radiol.2513071235
40. Jerbi M, Hidar S, Ziadi S, Khairi H (2006) Benign multicystic peritoneal mesothelioma. Int J Gynaecol Obstet 93:267–268. https://doi.org/10.1016/j.ijgo.2006.03.013
41. Diel J, Ortiz O, Losada RA, et al. (2001) The sacrum: pathologic spectrum, multimodality imaging, and subspecialty approach. Radiographics 21:83–104. https://doi.org/10.1148/radiographics.21.1.g01ja0883
42. Wells RG, Sty JR (1990) Imaging of sacrococcygeal germ cell tumors. Radiographics 10:701–713. https://doi.org/10.1148/radiographics.10.4.2165626
43. Farsad K, Kattapuram SV, Sacknoff R, Ono J, Nielsen GP (2009) Sacral chordoma. Radiographics 29:1525–1530. https://doi.org/10.1148/rg.295085215
44. Sciubba DM, Chi JH, Rhines LD, Gokaslan ZL (2008) Chordoma of the spinal column. Neurosurg Clin N Am 19:5–15. https://doi.org/10.1016/j.nec.2007.09.006
45. York JE, Kaczaraj A, Abi-Said D, et al. (1999) Sacral chordoma: 40-year experience at a major cancer center. Neurosurgery 44:74–79 (discussion 79–80)